Genetic basis of cardiac ion channel diseases

Koopmann, T.

Publication date
2008

Chapter 3

A mutation in the human cardiac sodium channel (E161K) contributes to sick sinus syndrome, conduction disease and Brugada syndrome in two families

Jeroen P.P. Smits*, Tamara T. Koopmann*, Ronald Wilders, Marieke W. Veldkamp, Tobias Opthof, Zahir A. Bhuiyan, Marcel M.A.M. Mannens, Jeffrey R. Balser, Hanno L. Tan, Connie R. Bezzina, Arthur A.M. Wilde

* These authors contributed equally to this study

J Mol Cell Cardiol. 2005;38:969-81

Editorial comment by Z.I. Zhu and C.E. Clancy: From mutation to clinical presentation: mechanisms in the black box.
J Mol Cell Cardiol. 2005;38:965-8

Abstract

Background Mutations in the gene encoding the human cardiac sodium channel (*SCN5A*) have been associated with three distinct cardiac arrhythmia disorders: the long QT syndrome, the Brugada syndrome and cardiac conduction disease. Here we report the biophysical features of a novel sodium channel mutation, E161K, which we identified in individuals of two non-related families with symptoms of bradycardia, sinus node dysfunction, generalised conduction disease and Brugada syndrome, or combinations thereof.

Methods and Results Wild-type (WT) or E161K sodium channel α-subunit and β-subunit were cotransfected into tsA201 cells to study the functional consequences of mutant sodium channels. Characterization of whole-cell sodium current (I_{Na}) using the whole cell patch-clamp technique revealed that the E161K mutation caused an almost threefold reduction in current density ($p<0.001$), and an 11.9 mV positive shift of the voltage-dependence of activation ($p<0.0001$). The inactivation properties of mutant and WT sodium channels were similar. These results suggest an overall reduction of E161K I_{Na}. Incorporation of the experimental findings into computational models demonstrate atrial and ventricular conduction slowing as well as a reduction in sinus rate by slowing of the diastolic depolarization rate and upstroke velocity of the sinus node action potential. This reduction in sinus rate was aggravated by application of acetylcholine, simulating the dominant vagal tone during night.

Conclusion Our experimental and computational analysis of the E161K mutation suggests that a loss of sodium channel function is not only associated with Brugada syndrome and conduction disease, but may also cause sinus node dysfunction in carriers of this mutation.

Keywords

Arrhythmia, sinus node dysfunction, Brugada syndrome, conduction disease, electrophysiology, ion channel, sodium channel, genetics, mutation

3.1 Introduction

Cardiac arrhythmias in the absence of structural abnormalities form an extending group of cardiac diseases. These so-called 'primary electrical diseases' of the heart are of a hereditary nature and can be associated with specific mutations in genes mostly encoding ion channel proteins.[1,2] The consequences of such mutations are alterations in the biophysical properties of ion channel proteins, which may affect normal cardiac electrophysiology and render the heart susceptible to the development of life-threatening arrhythmias.[1,2]

Mutations in the gene encoding the pore forming α-subunit of the human cardiac sodium channel (*SCN5A*) have been associated with a variety of cardiac rhythm disorders. The majority of sodium channel (hH1) mutations identified thus far, produce the long QT syndrome type 3 (LQT3), Brugada syndrome and cardiac conduction disease.[2] Albeit more rarely, other forms of arrhythmia syndromes have also been linked to mutations in this gene,[1-7] including acquired LQTS,[7] idiopathic ventricular fibrillation,[3] sick sinus syndrome[4,6] and atrial standstill.[5] Sinus node dysfunction has also been evidenced in patients with a sodium channel mutation that causally associated with LQT3.[8,9] Sinus node dysfunction in combination with QT-interval prolongation has also been reported due to a mutation in the gene *ANK2*, encoding ankyrin-B (LQT4[10-12]). An isolated case of sinus node dysfunction has been reported as a consequence of a *de novo* mutation in the *HCN4* gene encoding the pacemaker current I_f.[13]

With regards to *SCN5A* mutations, a general concept has emerged that links gain-of-function mutations to LQT3 and loss-of-function mutations to Brugada syndrome or conduction disease.[2] In this study we present a novel *SCN5A* mutation, E161K, which we identified in individuals from two non-related families with sinus node dysfunction as well as features of conduction disease and Brugada syndrome. By characterization of the clinical phenotype and the basic electrophysiological properties of E161K mutant Na^+ channels, along with computer simulations, we provide insight into the mechanisms underlying the complex clinical phenotype observed.

3.2 Materials and Methods

Clinical data

Informed consent was obtained from study participants according to the guidelines of the medical ethics committee of the hospital. Our study and all experiments conform to the Declaration of Helsinki. Subjects were evaluated by medical history, cardiac catheterization, magnetic resonance imaging (MRI) and echocardiograms. On a 12-lead electrocardiogram (ECG) the following ECG parameters were determined: heart rate, P wave duration (leads II and V1), PQ-, QRS-, and QTc-intervals (QTc was calculated according to Bazett's formula). J-point elevation was measured in leads V1 and V2 of the ECG. A flecainide test was performed in 2 members of family A and in 8 of family B (including B-II-9, B-III-14, B-III-15 and B-III-17, but not in B-III-13). This test is applied when patients are suspected of having Brugada syndrome because of J-point elevation on their baseline ECG, or because of suspicious family history. It consists of a challenge with flecainide administered intravenously (2 mg/kg; maximum dose 150 mg).[14] Also, 24-hour Holter recordings were obtained for 10 mutation carriers. For each

mutation carrier, Holter recordings from 2-3 patients matched for age and gender were obtained from hospital records to serve as controls. In this control group, there was no evidence for the presence of structural heart disease or medication that would affect heart rate. Additionally, the two index patients underwent a clinical electrophysiological study (EPS), testing the inducibility of ventricular arrhythmias, using up to 2 premature stimuli.

Sinus node dysfunction was considered if one of the following conditions was recorded at one or more occasions when inappropriate for the circumstances: (i) sinus bradycardia, (ii) sinus arrest or exit block, and (iii) combinations of sinoatrial (SA)-, and atrioventricular (AV)-conduction disturbances; these bradyarrhythmias often occurred in conjunction with paroxysmal atrial tachyarrhythmias.[15]

Mutation detection

Genomic DNA was extracted from peripheral blood lymphocytes using standard protocols. All exons of *SCN5A* and *HCN4* were amplified by PCR using primers located in flanking intronic sequences (listed in references [16] and [13], respectively), and sequenced directly for mutation screening. The coding region of connexin40 (Cx40) was screened by sequencing of PCR products generated with primers: 5'-GGGAGACGAAAGTTTTGGCAT-3' (F) and 5'-ATGCAGGGTG-GTCAGGAAGAT-3' (R), and 5'-GCTTCATTGTGGGCCAGTAC-3' (F) and 5'-GGTCCTGATCCTCC-CATAAAG-3' (R).

The presence of the nucleotide substitution leading to the E161K mutation in *SCN5A* was validated by restriction enzyme digestion using *Taq* I since this substitution abolished a recognition site for this enzyme. A control population of 100 individuals drawn from the same ethnic group (Dutch, Caucasian) was screened for the presence of this mutation in the same way.

SCN5A haplotype analysis

SCN5A haplotype analysis was carried out by genotyping two microsatellite markers, D3S1298 and D3S1100, which tightly flank the *SCN5A* gene using standard semi-automated methods.

Heterologous expression of the mutant and wild-type sodium channels

Mutant sodium channel cDNA was generated by site-directed mutagenesis on the pSP64T-hH1 plasmid followed by subcloning of the mutated cDNA into the *Hind* III-*Xba* I site of the mammalian expression vector pCGI (GFPIRS, for bicistronic expression of the channel protein and GFP reporter), as described previously.[17] E161K or wild-type sodium channel α-subunit construct (1 μg) was tranfected into tsA201 cells together with 1 μg hβ1-subunit construct (provided by AL George, Vanderbilt University, Nashville, TN) using lipofectamine (Gibco BRL, Life Technologies). Cells displaying green fluorescence 24-48 hours after transfection were used for electrophysiological experiments.

Electrophysiology

Sodium currents were measured in the whole-cell configuration of the patch-clamp technique using an Axopatch 200B amplifier (Axon Instruments Inc.). Currents were sampled at 20 kHz using a Digidata 1200 analog to digital board (Axon Instruments Inc.) and low-pass filtered at 2 kHz. Data acquisition was performed using pClamp 8.0.1 (Axon Instruments Inc.) and data were analyzed using Clampfit (Axon Instruments Inc.). Series resistance was compensated by ≈ 80%.

All experiments were performed at room temperature (21°C). The bath (external) solution contained (in mmol/L): NaCl 140, KCl 4.7, $CaCl_2$ 1.8, $MgCl_2$ 2.0, $NaHCO_3$ 4.3, Na_2HPO_4 1.4, glucose 11.0, HEPES 16.8, pH adjusted to 7.4 (NaOH). The pipette (internal) solution contained (in mmol/L): CsF 100, CsCl 40, EGTA 10, NaCl 10, $MgCl_2$ 2.0, HEPES 10, pH adjusted to 7.3 (NaOH).

Voltage protocols and data analysis

The voltage protocols used to determine voltage dependence of activation, steady-state inactivation, recovery from inactivation and development of slow inactivation are provided as insets in the relevant figures. Cycle time for each voltage protocol was 5 seconds.

Steady-state activation and inactivation curves were fit using the Boltzmann equation: $I/I_{max}=A/\{1.0+\exp[(V_{1/2}-V)/k]\}$ to determine the membrane potential for half-maximal (in)activation $V_{1/2}$ and the slope factor k. Recovery from inactivation was analyzed by fitting the data with a bi-exponential equation: $I/I_{max}= A_{fast}\,[1-\exp(-t/\tau_{fast})] + A_{slow}\,[1-\exp(-t/\tau_{slow})]$, where t is the time from onset of recovery and τ_{fast} and τ_{slow} are the fast and slow time constants of recovery from inactivation. Development of slow inactivation was analyzed by fitting the data with a mono-exponential function $I/I_{max}=Ae^{-t/\tau}$. The time course of inactivation was determined by fitting current decay with a two-exponential function: $I/I_{max}= A_f\exp(-t/\tau_f) + A_s\exp(-t/\tau_s)$, where A_f and A_s are fractions of fast and slowly inactivating components and τ_f and τ_s are the time constants of the fast and slowly inactivating components, respectively.

Computer simulations

The functional effects of the altered biophysical features of the mutant sodium channel on ventricular action potential propagation were tested by computer simulations using the single human ventricular cell model by Priebe and Beuckelmann.[18] As diagrammed in Figure 6A, individual myocytes were coupled into a linear strand of 80 cells with an intercellular coupling conductance G_c and a cytoplasmic resistivity of 150 Ω cm.[19] A propagating action potential was elicited by stimulating the strand at one end using a 2-ms, ≈20% suprathreshold stimulus current, and its conduction velocity was determined by monitoring the time required for conduction across the middle third of the strand. To obtain a conduction velocity of 65 cm/s during sinus rhythm as reported for human ventricles,[20] G_c was set to 6 μS. This value is well within in the estimated range of 3–12 μS for the gap junctional conductance between human ventricular myocytes.[19] To represent control individuals (non-carriers), no changes were made to the fast sodium current of the Priebe-Beuckelmann model, which has a maximum (fully-activated) conductance (G_{Na}) of 16 nS. To represent the heterozygous E161K mutant carriers, the model sodium current was separated into a component carried by wild-type channels and a component carried by E161K channels. The wild-type component had a maximum

conductance, whereas the mutant component had a maximum conductance of 3.2 nS (20% of control, thus accounting for the observed 2.5-fold reduction in current density for the E161K mutant channels) as well as an 11.9 mV shift in steady-state activation, as observed for the E161K mutant channels. In this implementation of the mutant channel properties, it is assumed that the relative changes that were observed at room temperature, i.e., a 2.5-fold reduction in current density and an 11.9 mV shift in steady-state activation of the E161K mutant vs. wild-type, also hold at the model temperature of 37°C. The minor change in the slope factor of the steady-state activation curve for the E161K channels was not incorporated into the model.

The functional effects of the altered biophysical features of the mutant sodium channel on atrial action potential propagation were assessed in a similar way, now using the single human atrial cell model by Courtemanche et al.[21] For this model, we increased its original value of G_{Na} by a factor of 3.8 in order to obtain a single cell upstroke velocity of ≈540 V/s, in accordance with data from patch clamp experiments on isolated human atrial myocytes obtained in our laboratory (Dr. Arie O. Verkerk, personal communication). For the atrial cell strand, we set G_c to 8 μS, which yields a conduction velocity of 84 cm/s, in accordance with the values of 88±3 cm/s[22] and 83±4 cm/s[23] reported for human atrium during sinus rhythm. It should be noted that conduction velocities >58 cm/s could not be obtained without increasing the original value of G_{Na}. Interestingly, in their simulations of atrial action potential propagation using the human atrial cell model by Nygren et al.,[24] Nygren and Giles also found that "the maximum permeability parameter of I_{Na} had to be increased by a factor 3.19 to reach a desired nominal conduction velocity of 60 cm/s".[25]

The effects of the altered biophysical features of the mutant sodium channel on SA node activity were tested by computer simulations using the model of a single peripheral SA nodal cell as introduced by Zhang et al.[26] and subsequently modified to allow for physiological control of intrinsic rate by application of acetylcholine (ACh).[27] The E161K mutation was incorporated into the model as set out above for the ventricular cell model.

Models were coded using Compaq Visual Fortran 6.6 and run on a 3-GHz Intel Pentium-4 processor workstation as a 32-bit Windows application, applying a simple and efficient Euler-type integration scheme with a 1-μs time step for simulations of atrial or ventricular action potential propagation and a 10-μs time step for simulation of the SA nodal action potential. The spatial discretization step in the strand simulations was 100 μm, i.e., the length of a single cell, which was treated as isopotential. All simulations were run for a sufficiently long time to reach steady-state behavior.

Statistical analysis

Data are expressed as mean±SEM. Statistical analysis of ECG and electrophysiological data was done using the unpaired Student's *t*-test. For analysis of the 24-hour ECG data a Wilcoxon test was used. A two-tailed probability value <0.05 was considered statistically significant.

3.3 Results

Genotype and haplotype analyses, and clinical phenotype

The index patients who, as evidenced by analysis of *SCN5A* haplotypes, originated from non-related families (referred to as families A and B, Figure 1) consulted their physician because of palpitations. Due to the fact that they had abnormal ECGs (Figure 2) and suspicious family histories, an inherited primary electrical disease of the heart was suspected. Affected patients had a complex clinical phenotype of conduction disease, Brugada syndrome and sick sinus syndrome. DNA sequencing of the *HCN4* gene in individual II-4 from family A (A-II-4) and individuals B-II-6, B-II-11 and B-II-17 from family B (Figure 1) uncovered no mutation in this gene. Since reduced expression of the cardiac gap junction protein connexin40, which is expressed in the conduction system and atria, has been associated with impaired conduction,[28] the gene encoding Cx40 was additionally screened and also revealed no mutation. Screening of the *SCN5A* gene in the same individuals identified a g>a substitution at nucleotide 481 in exon 4 in all individuals except B-II-6. This nucleotide substitution results in the replacement of the acidic residue glutamic acid at position 161 – located within the second transmembrane segment of the first domain of the channel – by the basic residue lysine (E161K). Testing of other family members identified more carriers of this mutation in both families (Figure 1). The mutation was not detected in 200 control chromosomes tested.

Family A

The index patient (Figure 1, A-II-4) is a 67 year old female who presented with palpitations due to sinus arrhythmia and occasional SA exit block. Examination of the ECG revealed a broad P-wave (120 ms), prolonged QRS duration (130 ms), and a coved type elevated ST-segment in leads V1 (2 mm) and V2 (3 mm) (Figure 2A). The coved type ST-segment elevations in leads V1 and V2 increased in magnitude (>2mm) after challenge with intravenous flecainide (Figure 2B). These ST-segment abnormalities fulfill the current ECG criteria for Brugada syndrome (type I).[14] During electrophysiological testing, non-sustained polymorphic ventricular tachycardia could be induced by two premature stimuli. Additional electrocardiographical investigation, by 24-hour Holter recordings, revealed the occurrence of SA exit block and sinus arrhythmia. Echocardiographic investigation and cardiac catheterization did not reveal any structural cardiac abnormalities. When the first-degree family members of the index patient were screened, her 62 year old asymptomatic sister (A-II-9) was also observed to have coved type ST-segment elevation on her ECG in lead V1 (1 mm). When challenged with intravenous flecainide, her ST-segment elevations also fulfilled the criteria for Brugada syndrome (2 mm coved-type ST-elevation in V2).

A total of 8 individuals from this family agreed to genetic and electrocardiographical examination. Besides the index patient and her sister, their brother was also found to be a carrier of the E161K mutation and showed the clinical features of Brugada syndrome. No cases of sudden cardiac death occurred in this family, the sister of the index patient (A-II-5) died of a malignancy.

Figure 1: Pedigrees of two non-related families in which the E161K cardiac sodium channel mutation was identified. Individuals marked with a plus sign are carriers of the E161K mutation. Individuals marked with a minus sign were tested for the presence of the E161K mutation and were found to be non-carriers. D3S1298 and D3S1100 are polymorphic microsatellite markers tightly flanking *SCN5A*. Arrows indicate the index patient of each family.

Family B

The index patient (Figure 1, B-III-23) is a 37 year old male who presented with palpitations. Examination of his ECG revealed features suggestive of Brugada syndrome (Figure 2C), SA node dysfunction (Figure 2D), and conduction abnormalities, including SA node exit block (Figure 2D), 1st degree A-V block with a PQ interval of 240 ms, incomplete right bundle branch block and saddle-back type J-point elevations in leads V1 (1 mm) and V2 (2 mm) (Figure 2C). The J-point elevation increased during challenge with flecainide. During electrophysiological investigation, abnormal sinus node function with a prolonged sinus node recovery time was observed and self-terminating polymorphic ventricular tachycardia could be induced. No structural cardiac abnormalities could be found using echocardiography or MRI. The patient was treated with an implantable cardioverter-defibrillator (ICD) with pacing mode. Two other family members (B-II-9 and B-II-11) had pacemakers implanted. No cases of sudden cardiac death occurred in this family, patient B-II-2 died of a malignancy, patient B-III-5 of meningitis, and the cause of death of individuals B-II-4 and B-II-19, at age 64, are unknown. Twenty-eight individuals from this family were genetically and electrocardiographically analyzed. The E161K mutation was identified in 11 family members (Figure 1B).

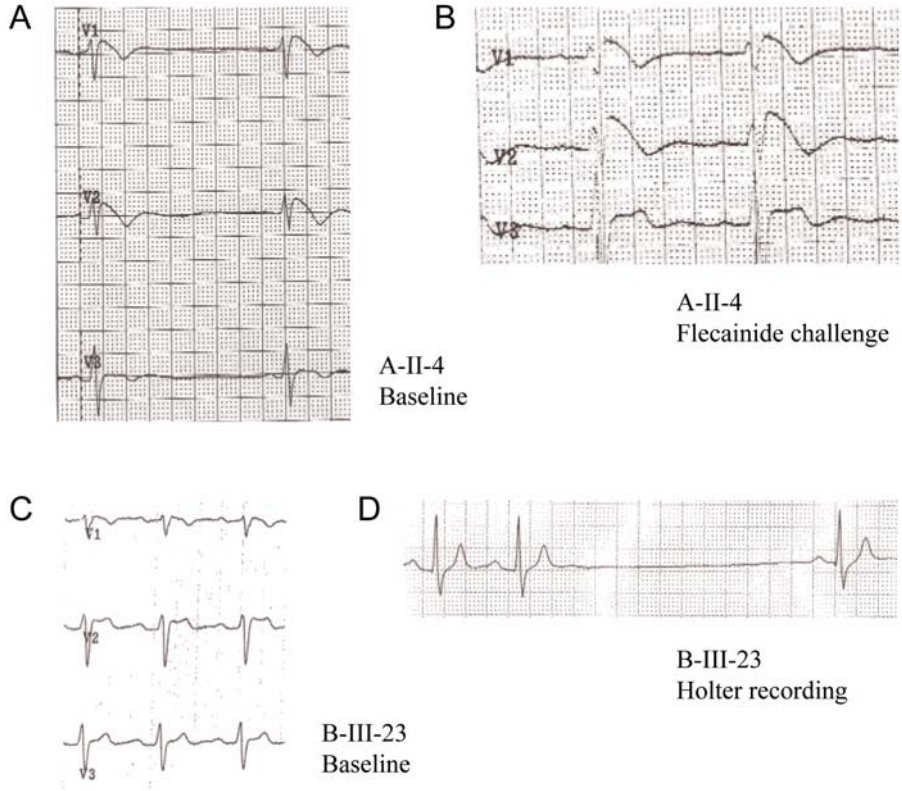

Figure 2: ECG data from the index patients. **A, B:** Right precordial leads, V1 to V3, of the index patient of family A (A-II-4), recorded during baseline conditions (A) and after flecainide challenge during which ST segment elevation increased (B). **C:** Right precordial leads V1 to V3 of the index patient of family B (B-III-23), recorded during baseline conditions. **D:** Holter recording of the same patient showing a sinus exit block.

Averaged ECG characteristics

The baseline electrocardiographic data of the 36 genotyped individuals from families A and B were pooled and averaged to allow comparison between mutation carriers and non-mutation carriers (Table 1). Carriers of the E161K mutation had ECG features typical for conduction disease, Brugada syndrome and sick sinus syndrome in various combinations and to variable degrees.

On average, E161K carriers were found to have longer P-wave, PQ- and QRS-intervals, indicative for conduction abnormalities. Average P-wave duration was 121±6 ms in mutation carriers and 98±3 ms ($p<0.0005$) in family members without the E161K mutation (23 ms increase). PQ-intervals were prolonged (>200 ms) in 4 out of 14 mutation carriers. On average, mutation carriers had a PQ-interval of 181±9 ms while that of family members without the E161K mutation was 156±6 ms ($p=0.015$). Widening of QRS-intervals (>100ms) was observed in 7 out of 14 E161K carriers, giving rise to an average value of 106±4 ms for mutation carriers vs. 88±2 ms for family members without the E161K mutation ($p=0.00015$). Sinus node dysfunction was observed in 8 out of 14 mutation carriers. Average heart rate (HR), obtained from baseline ECGs, was not significantly different between mutation carriers and family members without the E161K mutation (66±4 beats/min vs. 65±3 beats/min). In neither of the two families were spontaneous ventricular tachyarrhythmias documented. Spontaneous ST-segment elevation was observed in 7 out of 14 mutation carriers. The J-segment elevation in lead V1 was 0.6±0.2 mm for mutation carriers vs. 0.1±0.1 mm for non-mutation carriers ($p=0.0017$).

It should be noted that individual B-II-6, who does not carry the E161K mutation, did have spontaneous saddleback type ST-segment elevation that turned into a Type I ECG (coved) during flecainide challenge.[14] In addition, this patient also showed sinus bradycardia and sinus pauses, although less frequent than in E161K carriers.

Table 1. Averaged baseline ECG parameters from E161K mutation carriers and non-carriers.

	n	age (yrs)	gender (m:f)	HR beats/ min	P width lead II (ms)	PQ interval (ms)	QRS interval (ms)	QTc interval (ms)	ST elevation V1 (mm)
E161K carriers	14	47±4	8:6	66±4	121±6	181±9	106±4	409±8	0.6±0.2
non-carriers	22	45±4	12:10	65±3	98±3	156±6	88±2	403±6	0.1±0.1
p-value		ns	ns	ns	0.00049	0.015	0.0015	ns	0.0017

24-hour Holter recordings

Although mean heart rate obtained from baseline ECG's was not significantly different between mutation carriers and family members without the E161K mutation, analysis of 24-hour Holter recordings did show differences in heart rate. Of 7 mutation carriers, complete 24-hour Holter recordings were available from which maximum, minimum and mean heart rate during sinus rhythm were determined. Figure 3A shows that the averaged mean heart rate of E161K mutation carriers differed from that of 20 age- and gender-matched controls. With the exception of the time interval between 8am and 1pm, this difference was statistically significant ($p<0.05$). The absolute minimum heart rate, not necessarily during sinus rhythm, was additionally significantly lower in E161K mutation carriers (39 ± 1 beats/min) compared to controls (51 ± 0.6 beats/min ($p<0.001$) (Figure 3B). The maximum heart rate was not different, 133 ± 1.3 beats/min for E161K mutation carriers and 134 ± 0.8 beats/min (ns) for controls (Figure 3C). Of note, the incidence of signs of sick sinus syndrome in mutation carriers was particularly high at night.

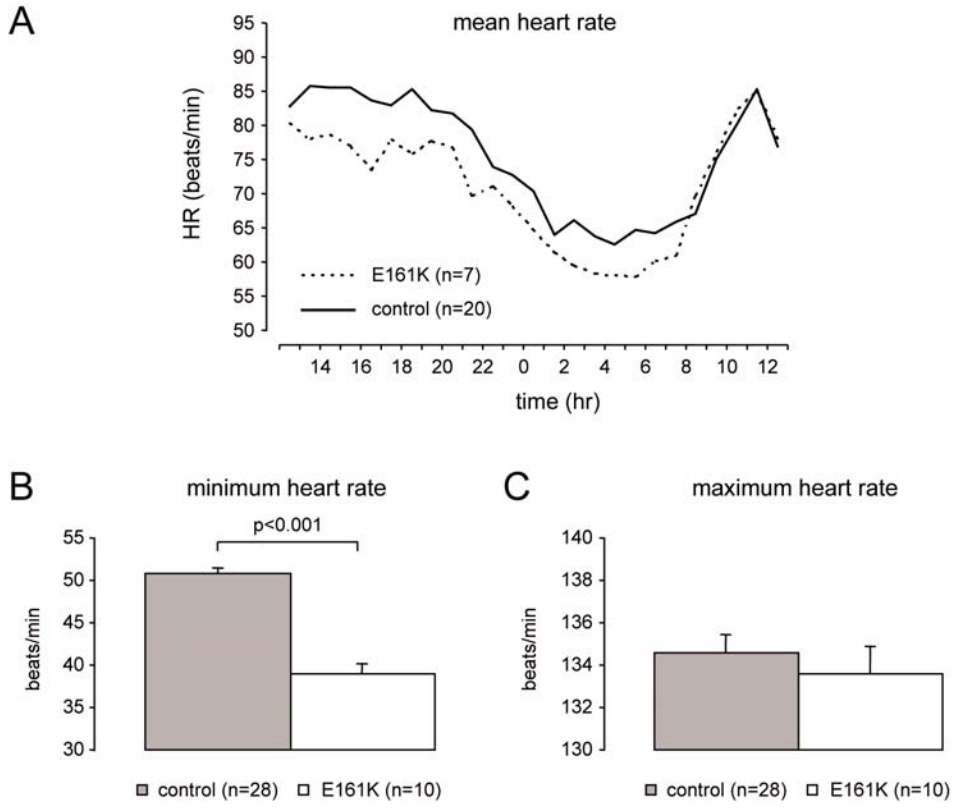

Figure 3: A: Mean heart-rate during 24 hour Holter monitoring of 7 E161K carriers from whom complete Holter recordings were available compared to 20 control individuals (non-family members). Except for the time interval between 8am and 1pm, E161K carriers had a significantly lower mean heart rate. **B, C:** Averaged absolute minimum (B) and maximum heart rate (C) for 10 E161K carriers and 28 control individuals (non-family members) as measured during Holter registration. For three E161K mutation carriers, the complete 24 hour Holter registrations were no longer available, only the final analysis reports were documented

Electrophysiology

To determine the functional consequences of the E161K sodium channel mutation, electrophysiological characteristics of mutant and WT sodium currents were studied in tsA201 cells. Figure 4 depicts examples of current traces (Figure 4A) and the averaged current-voltage (I-V) relationships (Figure 4B) of the WT and E161K channels, clearly showing that tsA201 cells transfected with E161K construct have a lower sodium current density. Peak I_{Na} for E161K sodium channels at –20 mV was reduced by a factor of 2.5 compared to WT channels ($p<0.001$). Fitting current decay with a bi-exponential function showed that the time constants of the fast and slow components were similar for WT and mutant channels (Figure 4C). The relative amplitude of the fast and slow components did not differ between WT and mutant channels.

Investigation of the voltage-dependence of activation and inactivation (Figure 5A) revealed an 11.9 mV positive shift of the half maximal activation potential ($V_{1/2}$) for E161K sodium channels (WT: $V_{1/2}$= –42.6±1.4 mV; E161K: –30.7±0.8 mV, $p<0.0001$). Also the steepness of the activation curve was slightly reduced (WT: k= 6.7±0.4 mV; E161K: k= 7.9±0.3 mV, $p<0.05$). Voltage dependence of steady state inactivation was not different (WT: $V_{1/2}$ = –89.4±1.2 mV, k= –4.9±0.3 mV vs. E161K: $V_{1/2}$ = –88.5±0.9 mV (ns), k= –4.4±0.1 mV (ns)). Recovery from inactivation (Figure 5B) and development of slow inactivation (Figure 5C) were not found to be different between E161K sodium channels compared to WT sodium channels (for values see legend).

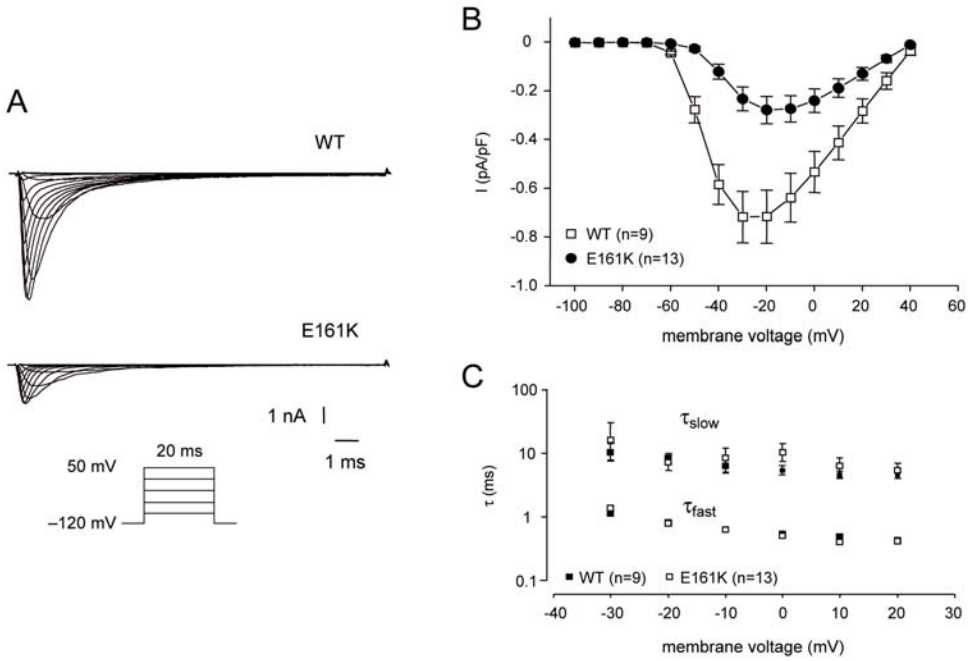

Figure 4: A: Representative examples of WT and E161K sodium current traces at various membrane potentials recorded from tsA201 cells. **B:** Average current-voltage relationships for WT and E161K sodium channels. Peak current amplitudes were significantly smaller for the E161K mutant as compared to WT. **C:** Fast and slow time constants of inactivation (τ_{fast} and τ_{slow}, respectively), obtained by fitting the sodium current decay with a bi-exponential function. No statistically significant differences were found.

Computer simulations

To investigate the effect of the E161K mutation on atrial and ventricular conduction, we studied action potential propagation in strands of human atrial or ventricular cells (Figure 6A), which we stimulated at one end at a frequency of 1.1 Hz, in accordance with the clinically observed heart rate of ≈66 beats/min (Table 1). As detailed in the Materials and Methods section, we selected intercellular coupling conductance values based on clinical data on atrial or ventricular conduction velocity during sinus rhythm.[20,22,23] Incorporation of the heterozygous E161K mutation by replacing half of the wild-type sodium current by 'E161K sodium current' (with a 2.5-fold reduction in current density and an 11.9 mV shift in steady-state activation) resulted in a 15% decrease in atrial conduction velocity from 84 to 72 cm/s (Figure 6B, left bars) and a 19% decrease in ventricular conduction velocity from 65 to 53 cm/s (Figure 6B, right bars). Such reduction would increase atrial and ventricular conduction time by 17 and 23%, respectively, which correlates reasonably well with the clinically observed ≈23% increase in P wave duration and ≈20% increase in QRS duration (Table 1).

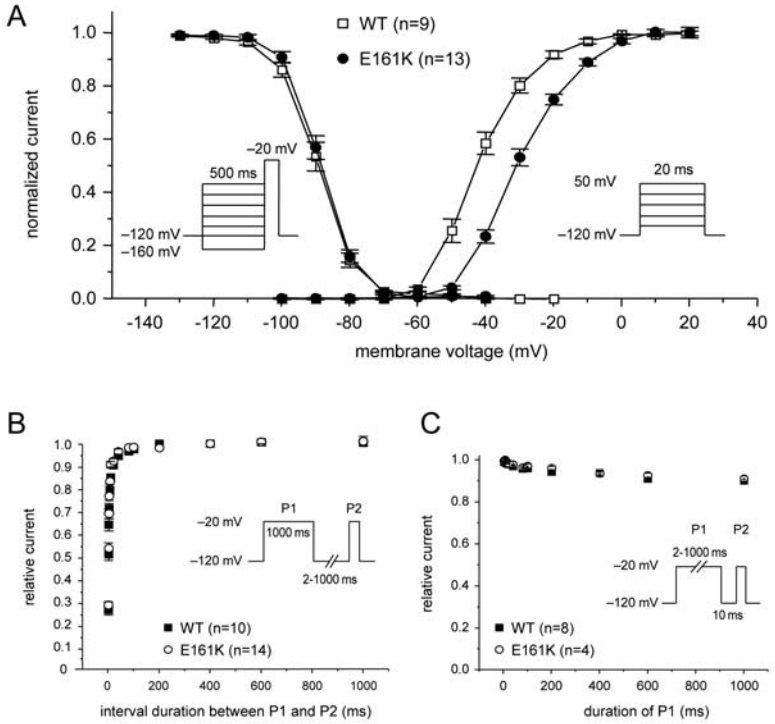

Figure 5: A: Voltage dependence of activation and inactivation of WT (n=9) and E161K (n=13) channels. Data were fitted with Boltzmann equations where $V_{1/2}$ is the half-maximal voltage and *k* is the slope factor. Values for activation were WT: $V_{1/2}$ = -42.6 ± 1.4 mV and *k* = 6.7 ± 0.4 mV vs. E161K: $V_{1/2}$ = -30.7 ± 0.8 mV ($p<0.0001$) and *k* = 7.9 ± 0.3 mV ($p<0.05$). Values for inactivation were WT: $V_{1/2}$ = -89.4 ± 1.2 mV and *k* = -4.9 ± 0.3 mV vs. E161K: $V_{1/2}$ = -88.5 ± 0.9 mV (ns) and *k* = -4.4 ± 0.1 mV (ns). **B:** Recovery from inactivation for WT and E161K mutant channels. Data were fitted with a biexponential function yielding the following amplitudes and recovery time constants: WT: A_{fast} = 0.95 ± 0.02 and τ_{fast} =1.9±0.2 ms vs. E161K : A_{fast} = 1.01 ± 0.03 and τ_{fast} = 1.8 ± 0.1 ms (ns); WT: A_{slow} = 0.18 ± 0.01 and τ_{slow} = 40.2 ± 3.6 ms vs. E161K : A_{slow} = 0.14 ± 0.01 and τ_{slow} = 38.0 ± 7.1 ms (ns) **C:** Development of slow inactivation for WT and E161K mutant channels. Abscissa: duration of P1, ordinate: amplitude of current elicited by P2 expressed as fraction of the amplitude of current elicited by P1. Data were fitted using a single exponential function giving a time constant of 361.8 ± 75.8 ms for WT (n=8) vs. 411.5 ± 132.9 ms for E161K (n=4) (ns).

To study the effect of the E161K mutation on the peripheral SA node, and the effects of subsequent vagal stimulation, we used the SA nodal cell model as designed by Zhang et al.[26,27] In this model one can test the autonomic control of the node by simulated application of ACh, which, in a concentration-dependent manner, depresses the L-type calcium current, shifts the activation curve of the hyperpolarization-activated current I_f, and activates the ACh-induced potassium current $I_{K,ACh}$. We compared action potential (AP) simulations in the presence of 100% normal sodium channels (labeled 'non-carriers') to simulations in which we replaced half of the sodium current by 'E161K sodium current' (with a 2.5-fold reduction in current density and an 11.9 mV shift in steady-state activation), thus representing the (heterozygous) E161K mutant carriers (labeled 'E161K carriers'). Like for the simulations of Figure 6, the minor change in the slope factor of the steady-state activation curve for the E161K channels was not incorporated into the model. Implementation of these altered properties gave rise to a reduction in sodium current during the upstroke of the AP and during the diastolic depolarization phase (Figure 7A). Together with a 2–3 mV shift in take-off potential to more positive values, as a result of the positive shift in the activation curve of the E161K channels, the resultant decrease in diastolic depolarization rate (DDR) and reduction in AP upstroke velocity, gave rise to a slight slowing of sinus rate (Figures 7A and 8A).

One may argue that our simulations of peripheral SA nodal activity tend to overemphasize the role of the sodium channel mutation because central SA nodal cells exhibit little or no sodium current. On the other hand, however, the electrotonic effects imposed by surrounding atrial cells would slow down diastolic depolarization in peripheral SA nodal cells, thereby increasing the effects of changes in sodium current, because these changes then occur on top of a smaller net membrane current. We refrained from using multicellular models of the sinus node and the sino-atrial interaction, because simulation results have shown to be critically dependent on the exact geometry and cell distribution,[30] which are a matter of ongoing debate.[31,32]

3.4 Discussion

In two non-related families, we have identified a novel *SCN5A* mutation, E161K, which segregated with features of cardiac conduction disease, Brugada syndrome and sick sinus syndrome. The clinical phenotype was highly variable as illustrated by the occurrence of different combinations of the three diseases (Figure 1).

The electrophysiological consequence of the E161K mutation, as measured in tsA201 cells, is a reduction in cardiac sodium current. This results from a reduced current density (Figure 4) and a positive shift in voltage dependence of activation (Figure 5A). As a consequence, E161K channels will provide less I_{Na} during the upstroke and phase 1 of the AP. This will reduce the AP upstroke velocity and slow down impulse propagation (Figure 6), and affect the AP configuration and the resulting surface ECG.

Simulated application of ACh, to mimic the heart rate depression during rest by tonic vagal activity and the signs of sick sinus syndrome, as observed at night in mutation carriers,[27,29] amplified the effects of the altered properties of the E161K mutation on sinus rate (Figures 7B and 8B). Although the E161K mutation gave rise to a slowing in sinus rate (SR) under baseline conditions (no Ach; Figures 7A and 8A) as well as in the presence of ACh (Figures 7B and 8B), this effect was far more pronounced in the latter (18% vs. 6%; Figure 7, top panels, and Figure 8).

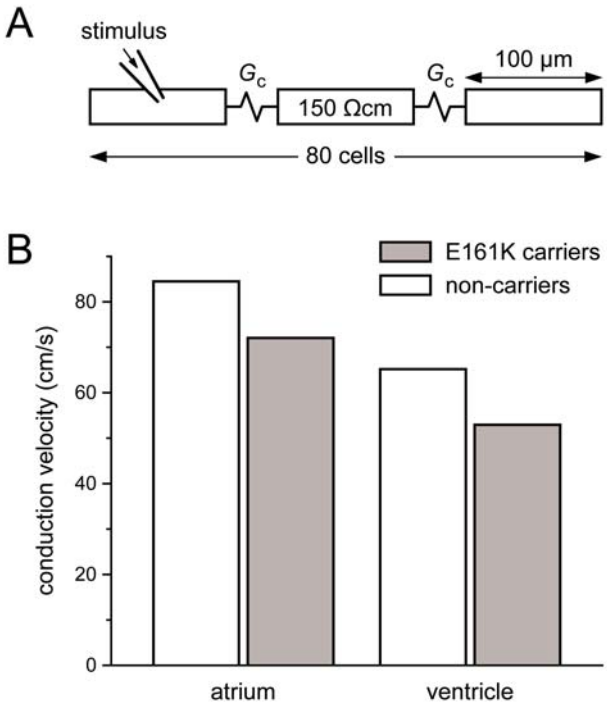

Figure 6: Simulated effects of E161K mutant biophysical properties on action potential propagation. **A:** Diagram of linear strand model. See Materials and Methods for details. **B:** Conduction velocity in linear strands of human atrial or ventricular cells (labelled 'atrium' and 'ventricle', respectively). Data for carriers of the E161K mutation appear as grey bars ('E161K carriers'), whereas the open bars show data for control individuals ('non-carriers').

This is mainly due to the larger decrease in DDR in the presence of ACh (27% vs. 8% under baseline conditions; Figure 8). The sodium current during the diastolic depolarization phase is reduced to approximately the same extent as in the absence of Ach (baseline conditions), but since this occurs on top of a smaller net membrane current, the effect on the rate of depolarization is more pronounced.

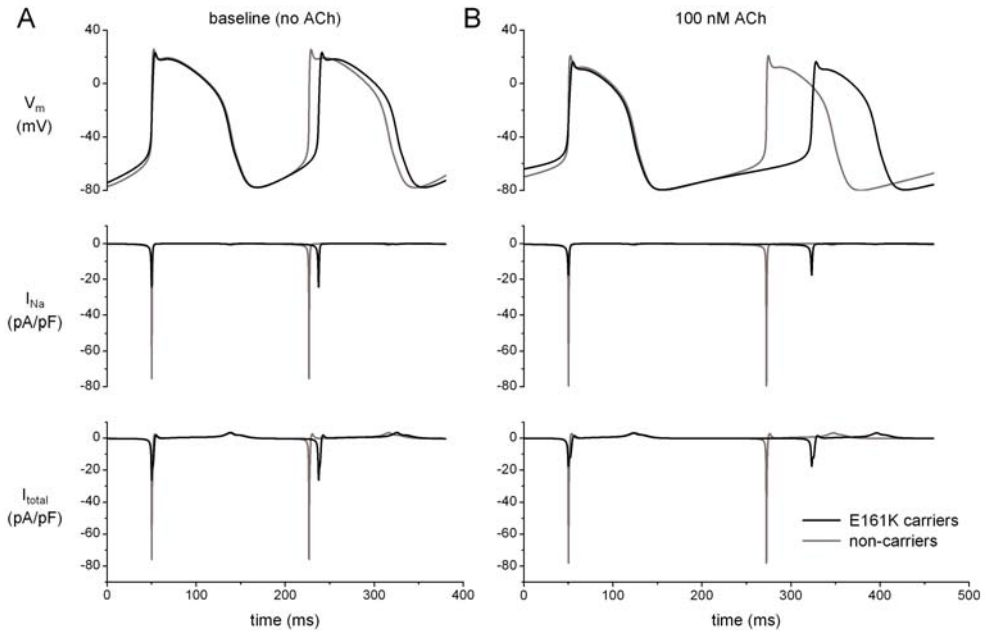

Figure 7: Simulated effects of E161K mutant biophysical properties on membrane voltage (V_m, top), sodium current (I_{Na}, middle), and net membrane current (I_{total}, bottom), during SA node spontaneous electrical activity. The black lines represent the (heterozygous) carriers of the E161K mutation ('E161K carriers'), whereas the grey lines represent control individuals ('non-carriers'). **A:** During baseline conditions (no ACh). **B:** After simulated application of 100 nM ACh.

Cardiac conduction disease

In the two families, individuals carrying the E161K mutation had broader P-waves and prolonged PQ and QRS-intervals as compared to non-carriers. The conduction disease in carriers of this mutation is attributable to the reduced conduction velocity of the cardiac AP, which results from the abnormal biophysical properties of the channel (Figure 6).

A reduction in upstroke velocity of the cardiac AP and a consequent slowing of conduction, due to loss-of-function *SCN5A* mutations, is not an uncommon mechanism in inherited cardiac conduction disease.[2] For example, in a computational cardiac model fiber, Tan et al.[33] have shown that a positive shift in voltage dependence of activation, as observed for the G514C sodium channel mutation, caused a reduction in AP upstroke velocity resulting in conduction delay. A positive shift in activation shifts the voltage threshold of sodium channel opening to more positive values, and will thus necessitate a greater voltage stimulus to depolarize the cells, slowing AP propagation. This, in combination with the reduction in I_{Na}, can also explain the abnormally widened P-wave and the longer PQ- and QRS-intervals in carriers of the E161K mutation (Figure 6).

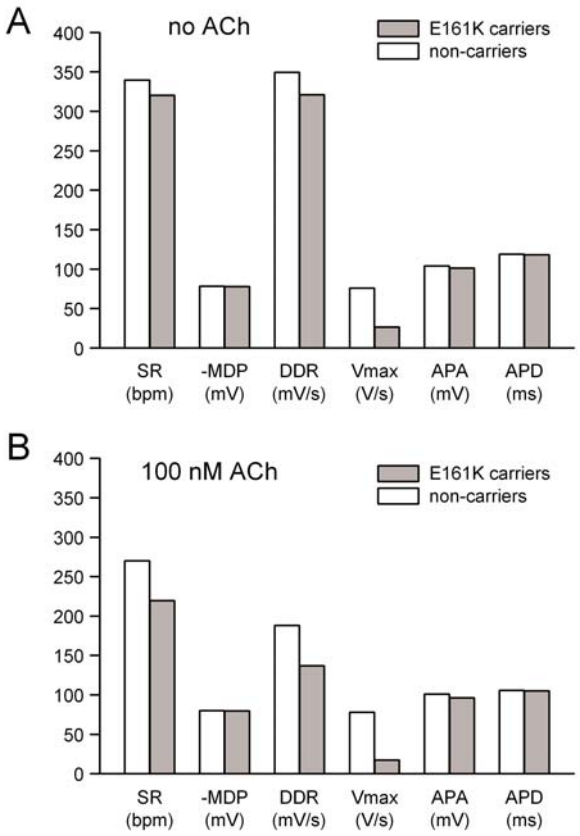

Figure 8: Simulated effects of the E161K mutant biophysical properties on sinoatrial node action potential parameters. The grey bars represent carriers of the E161K mutation ('E161K carriers'), whereas the open bars represent control individuals ('non-carriers'). SR=sinus rate, MDP=maximal diastolic potential, DDR=diastolic depolarization rate, defined as the rate of diastolic depolarization over a 10 ms interval starting at MDP + 1 mV, Vmax=action potential upstroke velocity, APA=action potential amplitude, APD=action potential duration at 100% repolarization. **A:** During baseline (no ACh). **B:** After simulated application of 100 nM ACh.

Impaired conduction can not only be caused by defects in the ion channels involved in cellular excitation, but also by defects in intercellular communication through gap junction channels. It has been demonstrated that P-wave duration, PQ interval, and QRS duration are significantly prolonged in Cx40-deficient mice.[34] However, screening of the gene encoding Cx40 did not reveal any genetic variation. This gene is therefore excluded as a possible modifier gene for the cardiac conduction disease phenotype in the investigated families. We did not screen the gene encoding connexin43 (Cx43), which is abundantly expressed in the ventricles.[19] However, genetic variation in this gene would specifically act on ventricular ECG parameters, as demonstrated by the observation that induced ablation of Cx43 in the adult mouse heart increased QRS duration without significant effects on the P wave or PQ interval.[35] Furthermore, both ECG parameters and activation maps of adult heterozygous Cx43 knockout mice do not differ from those of their control littermates.[36,37] Therefore, it is unlikely that the Cx43 gene acts as a modifier gene in the investigated families.

The Brugada syndrome

Two hypotheses have emerged to explain the Brugada syndrome ECG features and arrhythmias, both of which can result from reduction in I_{Na}. In the first hypothesis it is postulated that a reduction in I_{Na} during phase 0 of the AP causes a shortening of the AP because during the subsequent phase of early repolarization (phase 1) the presence of I_{to} may give rise to 'all or none repolarization'.[1,14,38] Because the epicardial layers of the heart have more I_{to} than endocardial cells, the epicardial AP will shorten to a greater extent. The resultant voltage gradient between epi- and endocardial layers of the heart may then give rise to ST-segment elevation.[1,14,38] The second hypothesis attributes the Brugada syndrome features to preferential conduction delay in the right ventricular outflow tract, for example due to a reduction in I_{Na}.[39] The sodium current reducing effects of the E161K mutation may explain the Brugada syndrome phenotype in the mutation carriers by either of these mechanisms.

The sick sinus syndrome

The sick sinus syndrome was evidenced by sinus bradycardia, SA exit block, complete heart block and paroxysmal atrial tachyarrhythmias. In addition, lower absolute heart rates and lower average heart rates in E161K mutation carriers as compared to healthy gender-and-age matched controls, were observed in 24-hour Holter recordings. The lower averaged heart rates were especially apparent during the night, while this difference disappeared in the early morning hours. This is probably due to the change in posture and the circadian variation in the autonomic nervous system that shows radical physiological changes during the time period directly after wakening, i.e. increase in catecholamine release.[40]

Two different mechanisms may underlie the sick sinus syndrome: (i) a hampered conduction between the SA node and the atria, due to an increased stimulus threshold in the atrial myocardium (the wider P waves are compatible with this), or (ii) a disorder of the SA node itself, as established for patient B-III-23 of family B during EPS. Although the role of I_{Na} in the SA node has been controversial, it is now well established that sodium channels contribute to SA node pacemaking in mammals.[40-44] To test for the effect of the reduced I_{Na} on intrinsic SA node activity, we used computer simulations that additionally allowed testing for effects of the parasympathetic nervous system. It was found that the reduced I_{Na} of the E161K mutant carriers gave rise to a slight reduction in upstroke velocity and DDR with consequent slowing of sinus rate (Figures 7 and 8). These effects were much more pronounced in the presence of ACh, simulating vagal dominance.[26,29] This is in accordance with the observations that significantly lower heart rates occurred at night and during the day except for the time interval between 8am and 1pm, when the sympathetic tone is dominant. This is supported by the fact that maximum heart rates were indistinguishable between mutation carriers and non-mutation carriers.

Genotype–phenotype relationship

Since compound heterozygous mutations in *SCN5A* have been linked to sick sinus syndrome in 3 families,[4] the involvement of a second *SCN5A* mutation in this family was excluded by analysis of *SCN5A* haplotypes (Figure 1). This possibility was further excluded by sequencing the entire *SCN5A* coding region in individuals B-II-6, B-II-11 and B-II-17, each bearing different *SCN5A* haplotypes; in this way, the *SCN5A* coding region of all *SCN5A* alleles segregating in affected individuals of generation II of this family were screened. No further *SCN5A* mutation was found in these individuals.

In spite of having saddleback type ST-segment elevations and a positive flecainide test, individual B-II-6 (family B) was not a carrier of the *SCN5A* E161K mutation. This is unusual, and only recently the first registration of two false positive sodium challenge tests, in this case using ajmaline, has been reported in two sisters who showed no evidence of Brugada syndrome and lacked the *SCN5A* (R367H) mutation presumed responsible for the disease in their (large) family.[45] In accordance with the speculations of the investigators involved in the latter study, various mechanisms could be responsible for the false positive flecainide test observed in individual B-II-6, among which is the occurrence of a second sodium channel mutation, possibly *de novo*, in this individual. However, sequencing of the entire coding region of *SCN5A* in this individual uncovered no such mutation. Another possibility could be that the E161K mutation is not responsible for the phenotype in this family. Two facts argue against this possibility: (i) the same mutation occurred in two non-related families presenting with the same combination of electrical phenotypes; in the two families, the mutation occurred on two different *SCN5A* haplotypes, suggesting an independent origin, and (ii) the mutation affects a highly conserved residue (E161) and the consequence of the mutation, i.e. the loss-of-function, are in line with what one expects of a mutation causing the electrical phenotypes observed in this family. Yet another possibility, which seems the most likely, is that an additional mutation, in a gene other than *SCN5A*, also contributes to the phenotype in this family. With regards to the involvement of other genes, a mutation in *HCN4*, the only other gene linked thus far to sick sinus syndrome, was also excluded. We suggest that a possible second gene in this family could be an important modifier of sodium channel function. Interestingly, a mutation in *SCN5A*, the only gene hitherto linked to the disorder, is only found in 15-30% of patients with the Brugada syndrome.[46-48] In the remaining patients, the disease is often also inherited, which suggests the involvement of other genes.[1,2]

In spite of being mutation carriers, individuals B-III-13, B-III-14, B-III-15 and B-III-17 did not display any phenotypic manifestations. This could be due to reduced penetrance, a common finding in primary electrical diseases in general and also in sodium channelopathy.[46,49] Other plausible explanations are that the expression of the disease is age-dependent, or that these individuals did not inherit the putative second gene mutation.

To conclude, the E161K mutation in the *SCN5A* gene is related to a clinical phenotype of cardiac conduction disease, sick sinus syndrome and Brugada syndrome with a variable clinical presentation. Loss-of-function *SCN5A* mutations have often been reported in association with the Brugada syndrome and cardiac conduction disease. This is however the first report of a loss-of-function *SCN5A* mutation in which the clinical phenotype is that of sick sinus syndrome and Brugada syndrome, and for which the biophysical properties have been characterized. Additionally, by using a computer model of SA nodal electrical activity we have provided novel insight into the mechanism underlying sick sinus syndrome due to loss-of-function mutation in *SCN5A*.

Acknowledgements

This study was financially supported by the Netherlands Heart Foundation (NHS grants 2000.059 to C.R.B. and A.A.M.W., and 2002B191 to H.L.T.), the Netherlands Organization for Scientific Research (grant 902-16-193 to A.A.M.W.), the Interuniversity Cardiology Institute of the Netherlands (project 27 to A.A.M.W.), a fellowship to H.L.T. by the Royal Netherlands Academy of Arts and Sciences (KNAW), and the Bekales Research Foundation (to C.R.B. and to H.L.T.)

Reference List

1. Roberts, R. & Brugada, R. Genetics and arrhythmias. *Annu. Rev. Med.* 54, 257-267 (2003).
2. Tan, H. L., Bezzina, C. R., Smits, J. P., Verkerk, A. O. & Wilde, A. A. Genetic control of sodium channel function. *Cardiovasc. Res.* 57, 961-973 (2003).
3. Akai, J. *et al.* A novel SCN5A mutation associated with idiopathic ventricular fibrillation without typical ECG findings of Brugada syndrome. *FEBS Lett.* 479, 29-34 (2000).
4. Benson, D. W. *et al.* Congenital sick sinus syndrome caused by recessive mutations in the cardiac sodium channel gene (SCN5A). *J Clin. Invest* 112, 1019-1028 (2003).
5. Groenewegen, W. A. *et al.* A cardiac sodium channel mutation cosegregates with a rare connexin40 genotype in familial atrial standstill. *Circ. Res.* 92, 14-22 (2003).
6. Kyndt, F., Schott, J. J., Probst, V., Chevallier, J. C. & Le Marec, H. A new *SCN5A* mutation associates with Brugada syndrome and sinus node dysfunction. *Circulation* 102 (Suppl II), II-281 (2000).
7. Makita, N. *et al.* Drug-induced long-QT syndrome associated with a subclinical SCN5A mutation. *Circulation* 106, 1269-1274 (2002).
8. Bezzina, C. *et al.* A single Na(+) channel mutation causing both long-QT and Brugada syndromes. *Circ. Res.* 85, 1206-1213 (1999).
9. Veldkamp, M. W. *et al.* Contribution of sodium channel mutations to bradycardia and sinus node dysfunction in LQT3 families. *Circ. Res.* 92, 976-983 (2003).
10. Mohler, P. J. *et al.* Ankyrin-B mutation causes type 4 long-QT cardiac arrhythmia and sudden cardiac death. *Nature* 421, 634-639 (2003).
11. Schott, J. J. *et al.* Mapping of a gene for long QT syndrome to chromosome 4q25-27. *Am. J. Hum. Genet.* 57, 1114-1122 (1995).
12. Schott, J. J. *et al.* Mutation in the ankyrin-B gene causes LQT syndrome and sinus node dysfunction. *Circulation* 106 (Suppl II), II-308 (2002).
13. Schulze-Bahr, E. *et al.* Pacemaker channel dysfunction in a patient with sinus node disease. *J. Clin. Invest* 111, 1537-1545 (2003).
14. Wilde, A. A. *et al.* Proposed diagnostic criteria for the Brugada syndrome. *Eur Heart J* 23, 1648-1654 (2002).
15. Olgin, J. E. & Zipes, D. P. *Heart Disease: A Texbook of Cardiovascular Medicine.* Braunwald, E., Zipes, D. P. & Libby, P. (eds.), pp. 815-899 (W.B. Saunders Company, Philadelphia, Pa,2001).
16. Wang, Q., Li, Z., Shen, J. & Keating, M. T. Genomic organization of the human SCN5A gene encoding the cardiac sodium channel. *Genomics* 34, 9-16 (1996).
17. Wedekind, H. *et al.* De novo mutation in the SCN5A gene associated with early onset of sudden infant death. *Circulation* 104, 1158-1164 (2001).
18. Priebe, L. & Beuckelmann, D. J. Simulation study of cellular electric properties in heart failure. *Circ. Res.* 82, 1206-1223 (1998).
19. Jongsma, H. J. & Wilders, R. Gap junctions in cardiovascular disease. *Circ. Res.* 86, 1193-1197 (2000).

20. Taggart, P. *et al.* Inhomogeneous transmural conduction during early ischaemia in patients with coronary artery disease. *J. Mol. Cell Cardiol.* 32, 621-630 (2000).

21. Courtemanche, M., Ramirez, R. J. & Nattel, S. Ionic mechanisms underlying human atrial action potential properties: insights from a mathematical model. *Am. J. Physiol* 275, H301-H321 (1998).

22. Hansson, A. *et al.* Right atrial free wall conduction velocity and degree of anisotropy in patients with stable sinus rhythm studied during open heart surgery. *Eur. Heart J.* 19, 293-300 (1998).

23. Kanagaratnam, P., Rothery, S., Patel, P., Severs, N. J. & Peters, N. S. Relative expression of immunolocalized connexins 40 and 43 correlates with human atrial conduction properties. *J. Am. Coll. Cardiol.* 39, 116-123 (2002).

24. Nygren, A. *et al.* Mathematical model of an adult human atrial cell: the role of K+ currents in repolarization. *Circ. Res.* 82, 63-81 (1998).

25. Nygren, A. & Giles, W. R. Mathematical simulation of slowing of cardiac conduction velocity by elevated extracellular. *Ann. Biomed. Eng* 28, 951-957 (2000).

26. Zhang, H. *et al.* Mathematical models of action potentials in the periphery and center of the rabbit sinoatrial node. *Am. J. Physiol Heart Circ. Physiol* 279, H397-H421 (2000).

27. Zhang, H., Holden, A. V., Noble, D. & Boyett, M. R. Analysis of the chronotropic effect of acetylcholine on sinoatrial node cells. *J. Cardiovasc. Electrophysiol.* 13, 465-474 (2002).

28. Nao, T. *et al.* Comparison of expression of connexin in right atrial myocardium in patients with chronic atrial fibrillation versus those in sinus rhythm. *Am. J. Cardiol.* 91, 678-683 (2003).

29. Katona, P. G., McLean, M., Dighton, D. H. & Guz, A. Sympathetic and parasympathetic cardiac control in athletes and nonathletes at rest. *J. Appl. Physiol* 52, 1652-1657 (1982).

30. Garny, A., Hunter, P. J., Noble, D., Boyett, M. R. & Kohl, P. *Proceedings of the 25th Annual International Conference of the IEEE Engineering in Medicine and Biology Society*., pp. 28-312003).

31. Verheijck, E. E., Wilders, R. & Bouman, L. N. Atrio-sinus interaction demonstrated by blockade of the rapid delayed rectifier current. *Circulation* 105, 880-885 (2002).

32. Zhang, H., Holden, A. V. & Boyett, M. R. Gradient model versus mosaic model of the sinoatrial node. *Circulation* 103, 584-588 (2001).

33. Tan, H. L. *et al.* A sodium-channel mutation causes isolated cardiac conduction disease. *Nature* 409, 1043-1047 (2001).

34. Kirchhoff, S. *et al.* Reduced cardiac conduction velocity and predisposition to arrhythmias in connexin40-deficient mice. *Curr. Biol.* 8, 299-302 (1998).

35. Eckardt, D. *et al.* Functional role of connexin43 gap junction channels in adult mouse heart assessed by inducible gene deletion. *J. Mol. Cell Cardiol.* 36, 101-110 (2004).

36. Morley, G. E. *et al.* Characterization of conduction in the ventricles of normal and heterozygous Cx43 knockout mice using optical mapping. *J. Cardiovasc. Electrophysiol.* 10, 1361-1375 (1999).

37. van Rijen, H. V. *et al.* Slow conduction and enhanced anisotropy increase the propensity for ventricular tachyarrhythmias in adult mice with induced deletion of connexin43. *Circulation* 109, 1048-1055 (2004).

38. Yan, G. X. & Antzelevitch, C. Cellular basis for the Brugada syndrome and other mechanisms of arrhythmogenesis associated with ST-segment elevation. *Circulation* 100, 1660-1666 (1999).

39. Tukkie, R. *et al.* Delay in right ventricular activation contributes to Brugada syndrome. *Circulation* 109, 1272-1277 (2004).

40. Opthof, T. The mammalian sinoatrial node. *Cardiovasc. Drugs Ther.* 1, 573-597 (1988).

41. Denyer, J. C. & Brown, H. F. Rabbit sino-atrial node cells: isolation and electrophysiological properties. *J. Physiol* 428, 405-424 (1990).

42. Irisawa, H., Brown, H. F. & Giles, W. Cardiac pacemaking in the sinoatrial node. *Physiol Rev.* 73, 197-227 (1993).

43. Kodama, I. *et al.* Regional differences in the role of the Ca2+ and Na+ currents in pacemaker activity in the sinoatrial node. *Am. J. Physiol* 272, H2793-H2806 (1997).

44. Muramatsu, H., Zou, A. R., Berkowitz, G. A. & Nathan, R. D. Characterization of a TTX-sensitive Na+ current in pacemaker cells isolated from rabbit sinoatrial node. *Am. J. Physiol* 270, H2108-H2119 (1996).

45. Hong, K. *et al.* Phenotypic characterization of a large European family with Brugada syndrome displaying a sudden unexpected death syndrome mutation in SCN5A. *J Cardiovasc. Electrophysiol.* 15, 64-69 (2004).

46. Priori, S. G. *et al.* Clinical and genetic heterogeneity of right bundle branch block and ST-segment elevation syndrome: A prospective evaluation of 52 families. *Circulation* 102, 2509-2515 (2000).

47. Schulze-Bahr, E. *et al.* Sodium channel gene (SCN5A) mutations in 44 index patients with Brugada syndrome: different incidences in familial and sporadic disease. *Hum. Mutat.* 21, 651-652 (2003).

48. Smits, J. P. *et al.* Genotype-phenotype relationship in Brugada syndrome: electrocardiographic features differentiate SCN5A-related patients from non-SCN5A-related patients. *J Am. Coll. Cardiol.* 40, 350-356 (2002).

49. Priori, S. G., Napolitano, C. & Schwartz, P. J. Low penetrance in the long-QT syndrome: clinical impact. *Circulation* 99, 529-533 (1999).